Enzyme Inhibition Hot Paper

DOI: 10.1002/ange.201306295

Development of an Activity-Based Probe and In Silico Design Reveal Highly Selective Inhibitors for Diacylglycerol Lipase-α in Brain**

*Marc P. Baggelaar, Freek J. Janssen, Annelot C. M. van Esbroeck, Hans den Dulk, Marco Allarà, Sascha Hoogendoorn, Ross McGuire, Bogdan I. Florea, Nico Meeuwenoord, Hans van den Elst, Gijsbert A. van der Marel, Jaap Brouwer, Vincenzo Di Marzo, Herman S. Overkleeft, and Mario van der Stelt**

Diacylglycerol lipase-α (DAGL-α) is an intracellular, multidomain protein responsible for the formation of the endocannabinoid 2-arachidonoylglycerol (2-AG) in the central nervous system.[1] 2-AG is an endogenous signaling lipid that interacts with the cannabinoid CB1 and CB2 receptors.[2] Little is known about the regulation of its biosynthetic pathway and it is largely unclear to what extent 2-AG is responsible for distinct cannabinoid CB1 receptor mediated biological processes. Selective inhibitors of DAGL-α may contribute to a more fundamental understanding of the physiological role of 2-AG and may serve as potential drug candidates for the treatment of obesity and neurodegenerative diseases.[3] Currently, there are no selective inhibitors and activity-based probes available for the study of DAGL-α.[4]

The identification of selective DAGL-α inhibitors is hampered by a lack of structural knowledge of the target, and a lack of assays that make use of endogenous DAGL-α activity in proteomes. No crystal structures are available and no homology models have been reported to aid hit identification and to guide optimization of the inhibitors. Determination of the selectivity of the inhibitors in native tissues is important because DAGL-α belongs to the serine hydrolase family, which contains more than 200 members with various physiological functions.[5] Fluorophosphonate (FP)-based probes are routinely employed in competitive activity-based protein profiling (ABPP) experiments to determine the selectivity of serine hydrolase inhibitors in complex proteomes. DAGL-α, however, does not react with these activity-based probes.[6] Therefore, a new probe that can label native DAGL-α would be of value for studying the potency and selectivity of novel DAGL-α inhibitors in brain proteomes. Here we present a strategy that combines a knowledge-based in silico design approach and the development of a novel activity-based probe (ABP), based on the nonselective DAGL-α inhibitor tetrahydrolipstatin (THL; also known as Orlistat, a drug used for the treatment of obesity). This strategy resulted in the rapid identification of DAGL-α inhibitors with a new chemotype and high selectivity in the brain proteome.

To identify novel DAGL-α inhibitors, we built a pharmacophore model based on THL using Discovery Studio Software Suite from Accelrys. Since THL can assume many different conformations, we searched the protein crystallographic database for crystal structures with a bioactive conformation for THL. A cocrystal structure of THL with fatty acid synthase (pdb-code: 2PX6) was identified (Figure 1 A)[7] that contains the same Ser-His-Asp catalytic triad and typical α/β hydrolase fold motif as DAGL-α. In this cocrystal structure, the nucleophilic Ser of the enzyme is covalently attached to the carbonyl moiety of the lactone. We reconstituted the ester to form the β-lactone to recover the active warhead of THL. After optimization of the geometry of the lactone, the resulting conformation was used to generate two pharmacophore models (Figure 1 B,C).

The essential features of both models are 1) a hydrogen-bond acceptor mimicking the carbonyl from the β-lactone; 2) hydrophobic hot spots corresponding to the lipophilic tails of THL; 3) a hydrogen-bond acceptor positioned at the *sn*-2 ester functionality; and 4) exclusion volumes representing the space occupied by the nucleophilic Ser and the backbone oxyanion hole residues in the active site of DAGL-α. Model 2 contained an additional hydrogen-bond donor feature derived from the leucinyl formamide moiety of THL. Using these models, we virtually screened a set of commercially available lipase inhibitors, which were mainly selected for their reactivity towards enzymes involved in endocannabinoid signaling (Table S1 in the Supporting Information). Analysis of the docking results revealed that two compounds ranked in the top five of both models, LEI103 (**1**) and LEI104

[*] M. Sc. M. P. Baggelaar, M. Sc. F. J. Janssen, A. C. M. van Esbroeck, M. Sc. S. Hoogendoorn, Dr. B. I. Florea, Ing. N. Meeuwenoord, Ing. H. van den Elst, Prof. Dr. G. A. van der Marel, Prof. Dr. H. S. Overkleeft, Dr. M. van der Stelt
Dept. of Bio-organic Synthesis, Leiden University
Einsteinweg 55, 2333 CC Leiden (The Netherlands)
E-mail: m.van.der.stelt@chem.leidenuniv.nl

M. Sc. M. Allarà, Prof. Dr. V. Di Marzo
Endocannabinoid Research Group
Institute of Biomolecular Chemistry, C.N.R.
Via Campi Flegrei 34, 80078, Pozzuoli (Italy)

Ing. H. den Dulk, Prof. Dr. J. Brouwer
Dept. of Molecular Genetics, Leiden University
Einsteinweg 55, 2333 CC Leiden (The Netherlands)

Dr. R. McGuire
Bioaxis Research
Bergse Heihoek 56, Berghem (The Netherlands)

[**] We would like to thank Prof. Dr. P. Doherty (King's College London (UK)) for his kind gift of wild type and DAGL-α knockout mouse brains.

Supporting information for this article is available on the WWW under http://dx.doi.org/10.1002/anie.201306295.

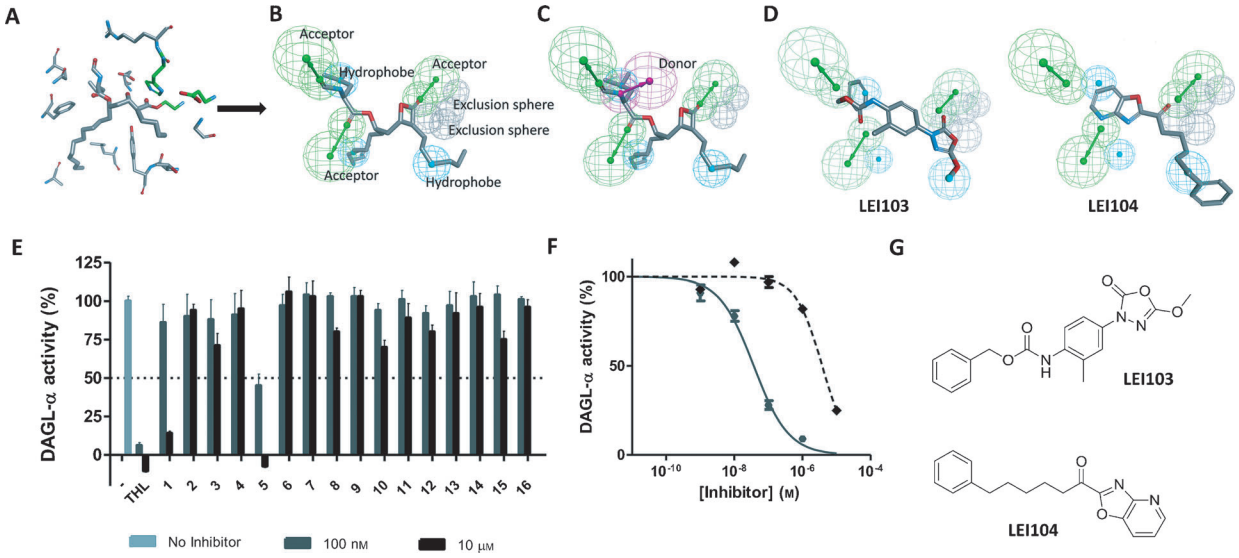

Figure 1. Identification of novel inhibitors for DAGL-α. A) Bioactive conformation of THL as retrieved from its known fatty acid synthase cocrystal structure (PDB code 2PX6). B) Pharmacophore model 1. C) Pharmacophore model 2. D) Docking results in pharmacophore model 1: highest ranked binding pose of LEI103 (4 features) and LEI104 (5 features). E) Screen of the targeted library using the colorimetric biochemical assay. Normalized residual activity was measured against hDAGL-α in HEK-293T cell membranes. F) Dose–response curves of LEI103 (black ◆) and LEI104 (gray ●) against hDAGL-α as determined with the colorimetric assay. LEI103: $IC_{50} = 3.8 \pm 0.4$ μM; LEI104: $IC_{50} = 37 \pm 5$ nM (±SEM, $n = 4$). G) Structures of LEI103 and LEI104.

(**5**; Figure 1D; Table S2 in the Supporting Information), whereas no binding mode was identified for compounds **3**, **4**, **7**–**11**, **13**, **14,** and **16** in either one or both models. This result demonstrates that the pharmacophore models were capable of discriminating between related structures of lipase inhibitors. Compound LEI103 is an oxadiazolone known to inhibit hormone-sensitive lipase,[8] whereas LEI104 is an α-ketoheterocycle that has been reported to inhibit fatty acid amide hydrolase (FAAH).[9] LEI104 has been shown to be active in in vivo models of antinociception through inhibiting FAAH.[10] Both hits represent new chemotypes that have not previously been shown to display DAGL-α inhibitory activity.

To validate our in silico hits, we used a colorimetric biochemical DAGL-α activity assay, which makes use of the hydrolysis of *para*-nitrophenylbutyrate by membrane preparations from HEK293T cells transiently transfected with human DAGL-α (hDAGL-α; Figure S2A–D in the Supporting Information).[11] Screening of the compound library against hDAGL-α (Figure 1E) confirmed LEI103 (**1**) and LEI104 (**5**) as the only compounds to inhibit hDAGL-α enzymatic activity by over 50% at 10 μM. Determination of the concentration–response dependency resulted in an IC_{50} of 37 ± 5 nM ($n = 4$) for LEI104, thus making it a hundred-fold more potent than LEI103 ($IC_{50} = 3.8 \pm 0.4$ μM; $n = 4$; Figure 1F). Of note, the reported DAGL-α inhibitor RHC80267[1a] (**16**) showed no inhibitory activity at 10 μM in our biochemical assay. In addition, we determined the activity of the hits in a radiometric assay using 1-[^{14}C]oleoyl-2-arachidonoylglycerol (1.0 mCi mmol^{-1}, 25 μM)[1a] as natural-like substrate. This assay confirmed that LEI104 is a more potent inhibitor of DAGL-α ($IC_{50} = 2.9 \pm 0.1$ μM) than LEI103 (37% inhibition at 10 μM).

To characterize the activity and selectivity of our hits on native DAGL-α in brain proteome, we employed competitive activity-based protein profiling (ABPP), which is an attractive and powerful chemical biology technique. It integrates organic chemistry, pharmacology, and chemical proteomics into the early stages of hit identification in the drug discovery process. It is unique in its ability to rapidly identify inhibitor activity and selectivity over large protein family classes in tissue samples.[5a] For this purpose, we designed MB064 as a novel activity-based probe (ABP) for DAGL-α based on the THL-analogue **31** (Scheme 1). An important consideration for choosing a THL-like compound as an ABP was that our pharmacophore models were also based on THL, thereby potentially leading to the identification of hits with the same off-target activities as THL. A THL-based ABP will enable us to detect these off-target activities as early as possible and to select the optimal hit. Compound **31** contains an alkyne for conjugation to a fluorophore and relies on a β-lactone warhead that forms a covalent bond with the catalytic nucleophilic serine. This principle has been used previously with bacterial, plant, and mammalian enzymes that share an α,β-hydrolase fold motif.[12] MB064 was synthesized following an established strategy.[13] The lactone ring was constructed using a tandem Mukaiyama aldol lactonization, yielding a (10:1 *anti*/*syn*) mixture of diastereomers, with a total selectivity for the *trans*-β-lactone. After removal of the TBS group, the diastereomers could be separated by column chromatography over silica gel. *N*-Formyl-L-leucine was introduced by a Mitsunobu reaction, inverting the δ-stereocenter towards the desired configuration. Coupling with a fluorophore (azido bodipy acid)[14] by using a copper catalyzed click reaction resulted in MB064, the first DAGL-

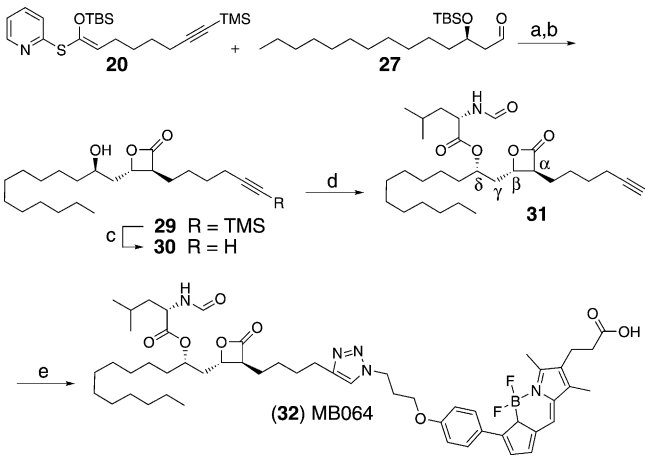

Scheme 1. Reagents and conditions: a) $ZnCl_2$, CH_2Cl_2, d.r. 1:10, 50%; b) HF, CH_3CN, 0°C, 91%; c) 2,6-lutidine/acetone/H_2O (0.1:1:1), $AgNO_3$, 79%; d) *N*-formyl-L-leucine, PPh_3, DIAD, THF, 30%; e) sodium ascorbate, $CuSO_4$, H_2O, CH_2Cl_2, 40%. DIAD = Diisopropyl azodicarboxylate. TBS = *tert*-butyldimethylsilyl, TMS = trimethylsilyl.

α sensitive ABP, (Scheme 1), which gave an IC_{50} of 6.0 ± 1.0 nM ($n = 4$) in the colorimetric assay.

To validate MB064 as a DAGL-α sensitive ABP, different hDAGL-α constructs were transiently transfected into HEK293T cells (Figure 2A). Incubation of the membrane fractions of hDAGL-α-FLAG transfected cells with MB064, followed by SDS-PAGE and fluorescence scanning revealed seven fluorescence signals (Figure 2B). The signal at approximately 120 kDa, which corresponded to the molecular mass of hDAGL-α, overlapped with a band visualized by the FLAG-tag antibody and was absent in mock-transfected cells. Preincubation with THL (10 μM) blocked enzymatic activity and nonspecific labeling. Site-directed mutagenesis of the catalytic DAGL-α nucleophile Ser472 into an alanine abolished the labeling of the proteins with MB064, thereby excluding enzymatic activity in the biochemical assay, and no band at around 120 kD was observed. hDAGL-α protein expression was not altered by the mutagenesis as determined with the FLAG-tag antibody (Figure 2A,B). Finally, we made a C-terminal deletion construct of hDAGL-α that was missing amino acids 688–1042. This mutant enzyme was still active as confirmed by our biochemical assay and was also labeled by MB064. Together, these data demonstrate that MB064 can efficiently label active hDAGL-α by forming a covalent bond with Ser472.

To determine whether our probe was able to react with native DAGL-α, we incubated MB064 with mouse membrane proteomes from different tissues (brain, heart, lung, testes, kidney, and liver). The highest DAGL-α activity was found in brain proteome, with negligible activity in the other tissues. MB064 labeled at least eight different proteins in brain (Figures 2C and 3A), and this labeling was prevented (or reduced to a large extent) by preincubation with THL (20 μM; Figure 3A). A distinct fluorescent band at approximately 120 kD was observed; this band could not be observed when the brain membrane proteome was incubated with TAMRA-FP. Of note, MB064 showed a much more restricted labeling profile than TAMRA-FP. In brain membrane proteomes from DAGL-α knockout mice, no specific band at around 120 kD was found (Figure 2C). Incubation of mouse brain lysate proteomes with MB064 led to the labeling of several proteins, but no specific signal at around 120 kD was detected (Figure S3 in the Supporting Information). This result is in line with the fact that DAGL-α resides in membranes. Finally, we detected mouse DAGL-α protein and eleven other proteins (Table 1) in a pull down experiment, using streptavidin beads and a biotinylated THL derivative, MB077, followed by tryptic digestion and mass spectrometric analysis of the isolated peptides. These proteins were not identified when the brain membrane proteome was preincubated with THL. Our proteomics experiment confirmed that THL reacts with several structural proteins (such as tubulin), glyceraldehyde-3-phosphate dehydrogenase, and lipid metabolizing enzymes (for example ABHD16a and platelet-activating factor acetylhydrolase), as reported.[6,13] We conclude that MB064 is able to visualize and detect DAGL-α in the mouse brain membrane proteome, and confirm that THL is a nonselective inhibitor of DAGL-α in mouse brain.

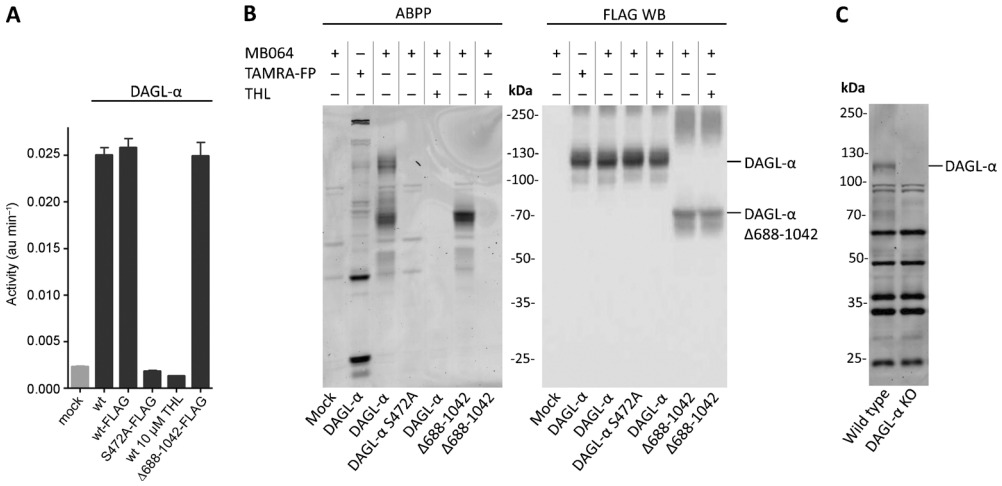

Figure 2. Validation of MB064 as a DAGL-α ABP. A) Activity, as measured with the colorimetric assay, of different hDAGL-α constructs transiently transfected into HEK-293T cells. Mock membranes and different constructs measured at the same protein concentration (1 μg μL^{-1}), uncorrected activity shown (± SEM, $n = 4$). B) ABPP using MB064 (250 nM) with different hDAGL-α constructs at the same protein concentration (2 μg μL^{-1}), and Western blot of the ABPP gel using an anti-FLAG antibody. C) ABPP using MB064 (250 nM) in brain membrane proteomes of wild type and DAGL-α knockout (KO) mice.

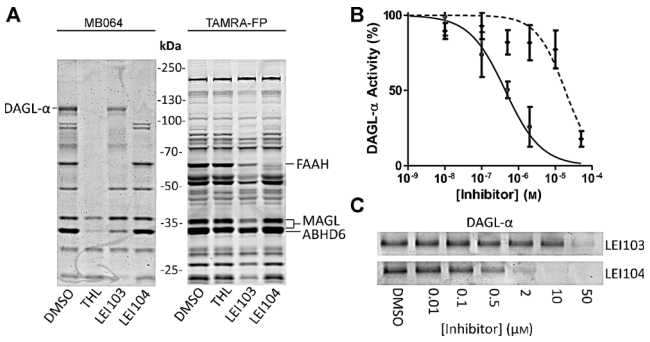

Figure 3. Selectivity profile and activity of LEI103 and LEI104 in the mouse brain membrane proteome. A) Competitive ABPP with the DAGL-α inhibitors THL, LEI103, and LEI104 (20 μM) using ABPs MB064 and carboxytetramethylrhodamine fluorophosphonate (TAMRA-FP) in mouse brain membrane proteome. B) Dose–response curves for DAGL-α inhibition by LEI103 (black -----◆-----) and LEI104 (gray ——●——) as measured by competitive ABPP with ABP MB064 (± SEM, $n = 3$). C) Concentration dependent inhibition of DAGL-α in the mouse brain membrane proteome.

Table 1: Proteins identified with MB077.

Proteins
tubulin beta
visinin-like protein 1
40S ribosomal protein S6
actin
glyceraldehyde-3-phosphate dehydrogenase
myelin basic protein
histone H2B type 1-M
ATP synthase subunit α
Sn1-specific diacylglycerol hydrolase α
abhydrolase domain containing protein 16A
monoacylglycerol hydrolase ABHD6
platelet-activating factor acetylhydrolase

ABPP experiment with LEI103 and LEI104 at 20 μM using mouse brain membrane proteome (Figure 3A). LEI103 prevented the labeling of six proteins by MB064, whereas LEI104 was much more selective and completely blocked the labeling of DAGL-α. This indicates that LEI103 has a similar off-target profile to that of THL. Other hits from the library screen did not inhibit DAGL-α (Figure S4 in the Supporting Information). LEI104 inhibited DAGL-α labeling with an IC_{50} of 450 ± 104 nM ($n = 3$), thereby making it approximately 40-fold more potent than LEI103 ($IC_{50} = 18 \pm 5$ μM; $n = 3$; Figure 3B). In addition, we performed a comparative ABPP experiment with TAMRA-FP to obtain a selectivity profile for our hits in the serine hydrolase family (Figure 3A). We observed that LEI103 inhibited several proteins, whereas LEI104 abolished only one signal at approximately 64 kD, which corresponded to FAAH.[10d] These results demonstrate that an ABP based on a pharmacophore model is highly useful for selecting and prioritizing hits found with the model, because it can rapidly detect potential off-target activities of these hits in the proteome that share a similar pharmacophore.

Based on its activity and selectivity profile, we decided to test LEI104 in intact cells. We incubated LEI104 (20 μM) or vehicle with intact SHSY5Y cells, stimulated them with ionomycin (3 μM), and measured 2-AG levels after 20 min.[1a] The 2-AG levels were significantly lower (−46%) in the treated cells compared with the control cells. This demonstrates that LEI104 is cell permeable and able to inhibit stimulus-induced 2-AG formation by DAGL-α in living cells. In conclusion, LEI104 represents a novel potent and selective chemotype for DAGL-α inhibition.

We performed a preliminary structure–activity relationship study of LEI104 with hDAGL-α using the colorimetric assay. Replacement of the isoxazolepyridine heterocycle with a benzoxazole led to a 100-fold loss in activity, thus indicating that the pyridine nitrogen could form a potentially important interaction with the active site of the enzyme (see the Supporting Information for synthesis).[9] Reduction of the α-keto group to the alcohol abolished all activity, a result in line with the assumption that this group functions as an electrophilic trap for the catalytic Ser472.

To understand the interaction of LEI104 with hDAGL-α at a molecular level, we developed a homology model of DAGL-α (see the Supporting Information). The model represents the typical α,β-hydrolase fold and has the catalytic triad (Ser472, His650, and Asp524) appropriately aligned in the binding cavity (Figure 4). The tetrahedral transition state of LEI104, which is formed through the nucleophilic attack of Ser472 on the α-carbonyl, was minimized and subjected to a short molecular dynamics refinement. According to our model, the oxyanion intermediate is stabilized by the backbone N–H of the residue adjacent to the catalytic serine, Leu473. In addition, both the side chain O–H and the backbone N–H of Thr400 are observed to make hydrogen bonds with the oxyanion. The oxazole nitrogen of LEI104 formed hydrogen-bond interactions with His650 and the pyridine nitrogen showed hydrogen-bond interactions with His471, both of which could further stabilize the transition state, while the hydrophobic pocket lined with

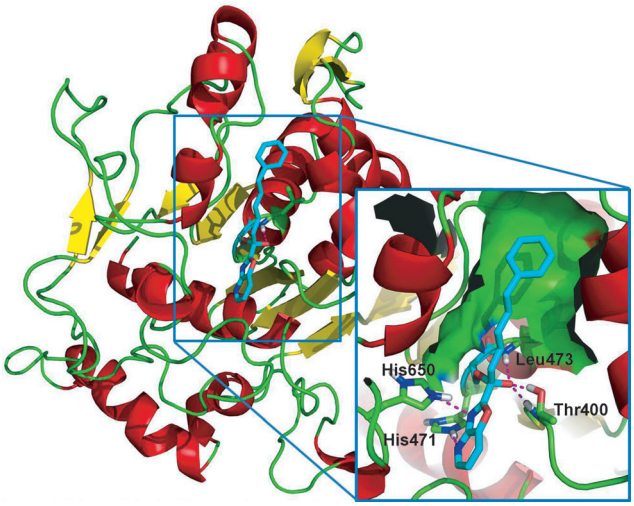

Figure 4. Binding pose of LEI104 (cyan) in a homology model of hDAGL-α.

aliphatic amino acids accommodated the flexible acyl chain of LEI104. This proposed binding mode is consistent with our observed structure–activity relationships. This model also provides a clear view of the opportunities to improve the potency and selectivity over FAAH. Since FAAH is the main enzyme responsible for the degradation of another important endocannabinoid, anandamide (AEA), its inhibition will lead to an upregulation of AEA levels.

To conclude, we have demonstrated the power of combining a pharmacophore-based in silico screening approach with ABPP-based chemoproteomics to identify and profile a novel chemotype for DAGL-α inhibition. Using an existing drug (THL) as a common starting point for the generation of both a pharmacophore model and an activity-based probe, we were able to rapidly identify the α-ketoheterocycle LEI104 as a highly selective DAGL-α inhibitor. It is anticipated that the α-ketoheterocycle class will provide an excellent lead series for dissecting 2-AG- and AEA-mediated cannabinoid CB1 signaling and for the development of in vivo active and selective DAGL-α inhibitors, because these compounds 1) have a clearly defined scaffold with excellent physicochemical properties; 2) are not based on the natural substrate and do not contain known toxicophores (for example fluorophosponate);[4b] 3) are plasma membrane permeable; 4) are highly selective; 5) do not form irreversible covalent bonds,[10] which could lead to problems with immunogenicity; and 6) have been shown to be bioavailable and active in animal models.[10] Finally, our probe and the α-ketoheterocycles, together with structural insights provided by the DAGL-α homology model, may serve as a basis for the development of new therapeutics that can be used to study and treat diseases such as obesity and neurodegeneration. These studies are currently in progress.

Received: July 19, 2013
Revised: September 11, 2013

Keywords: activity-based probe · drug discovery · endocannabinoid · hydrolases · proteomics

[1] a) T. Bisogno, F. Howell, G. Williams, A. Minassi, M. G. Cascio, A. Ligresti, I. Matias, A. Schiano-Moriello, P. Paul, E. J. Williams, U. Gangadharan, C. Hobbs, V. Di Marzo, P. Doherty, *J. Cell Biol.* **2003**, *163*, 463–468; b) M. Reisenberg, P. K. Singh, G. Williams, P. Doherty, *Philos. Trans. R. Soc. London Ser. B* **2012**, *367*, 3264–3275.

[2] I. Katona, T. F. Freund, *Annu. Rev. Neurosci.* **2012**, *35*, 529.

[3] a) V. Di Marzo, *Nat. Neurosci.* **2011**, *14*, 9–15; b) D. K. Nomura, B. E. Morrison, J. L. Blankman, J. Z. Long, S. G. Kinsey, M. C. Marcondes, A. M. Ward, Y. K. Hahn, A. H. Lichtman, B. Conti, B. F. Cravatt, *Science* **2011**, *334*, 809–813.

[4] a) T. Bisogno, J. J. Burston, R. Rai, M. Allara, B. Saha, A. Mahadevan, R. K. Razdan, J. L. Wiley, V. Di Marzo, *ChemMedChem* **2009**, *4*, 946–950; b) T. Bisogno, M. G. Cascio, B. Saha, A. Mahadevan, P. Urbani, A. Minassi, G. Appendino, C. Saturnino, B. Martin, R. Razdan, V. Di Marzo, *Biochim. Biophys. Acta Mol. Cell Biol. Lipids* **2006**, *1761*, 205–212; c) M. Johnston, S. R. Bhatt, S. Sikka, R. W. Mercier, J. M. West, A. Makriyannis, S. J. Gatley, R. I. Duclos, Jr., *Bioorg. Med. Chem. Lett.* **2012**, *22*, 4585–4592; d) G. Ortar, T. Bisogno, A. Ligresti, E. Morera, M. Nalli, V. Di Marzo, *J. Med. Chem.* **2008**, *51*, 6970–6979; e) K. L. Hsu, K. Tsuboi, A. Adibekian, H. Pugh, K. Masuda, B. F. Cravatt, *Nat. Chem. Biol.* **2012**, *8*, 999–1007; f) W. R. Marrs, J. L. Blankman, E. A. Horne, A. Thomazeau, Y. H. Lin, J. Coy, A. L. Bodor, G. G. Muccioli, S. S. Hu, G. Woodruff, S. Fung, M. Lafourcade, J. P. Alexander, J. Z. Long, W. Li, C. Xu, T. Moller, K. Mackie, O. J. Manzoni, B. F. Cravatt, N. Stella, *Nat. Neurosci.* **2010**, *13*, 951–957; g) T. Bisogno, A. Mahadevan, R. Coccurello, J. W. Chang, M. Allara, Y. Chen, G. Giacovazzo, A. Lichtman, B. Cravatt, A. Moles, V. Di Marzo, *Br. J. Pharmacol.* **2013**, *169*, 784–793.

[5] a) R. E. Moellering, B. F. Cravatt, *Chem. Biol.* **2012**, *19*, 11–22; b) J. Z. Long, B. F. Cravatt, *Chem. Rev.* **2011**, *111*, 6022–6063.

[6] H. S. Hoover, J. L. Blankman, S. Niessen, B. F. Cravatt, *Bioorg. Med. Chem. Lett.* **2008**, *18*, 5838–5841.

[7] C. W. t. Pemble, L. C. Johnson, S. J. Kridel, W. T. Lowther, *Nat. Struct. Mol. Biol.* **2007**, *14*, 704–709.

[8] Y. B. Ali, R. Verger, F. Carriere, S. Petry, G. Muller, A. Abousalham, *Biochimie* **2012**, *94*, 137–145.

[9] D. L. Boger, H. Sato, A. E. Lerner, M. P. Hedrick, R. A. Fecik, H. Miyauchi, G. D. Wilkie, B. J. Austin, M. P. Patricelli, B. F. Cravatt, *Proc. Natl. Acad. Sci. USA* **2000**, *97*, 5044–5049.

[10] a) A. H. Lichtman, D. Leung, C. C. Shelton, A. Saghatelian, C. Hardouin, D. L. Boger, B. F. Cravatt, *J. Pharmacol. Exp. Ther.* **2004**, *311*, 441–448; b) J. K. DeMartino, J. Garfunkle, D. G. Hochstatter, B. F. Cravatt, D. L. Boger, *Bioorg. Med. Chem. Lett.* **2008**, *18*, 5842–5846; c) D. L. Boger, H. Miyauchi, M. P. Hedrick, *Bioorg. Med. Chem. Lett.* **2001**, *11*, 1517–1520; d) D. Leung, C. Hardouin, D. L. Boger, B. F. Cravatt, *Nat. Biotechnol.* **2003**, *21*, 687–691.

[11] D. L. Pedicord, M. J. Flynn, C. Fanslau, M. Miranda, L. Hunihan, B. J. Robertson, B. C. Pearce, X. C. Yu, R. S. Westphal, Y. Blat, *Biochem. Biophys. Res. Commun.* **2011**, *411*, 809–814.

[12] a) M. Rusch, T. J. Zimmermann, M. Burger, F. J. Dekker, K. Gormer, G. Triola, A. Brockmeyer, P. Janning, T. Bottcher, S. A. Sieber, I. R. Vetter, C. Hedberg, H. Waldmann, *Angew. Chem.* **2011**, *123*, 10012–10016; *Angew. Chem. Int. Ed.* **2011**, *50*, 9838–9842; b) C. Hedberg, F. J. Dekker, M. Rusch, S. Renner, S. Wetzel, N. Vartak, C. Gerding-Reimers, R. S. Bon, P. I. Bastiaens, H. Waldmann, *Angew. Chem.* **2011**, *123*, 10006–10011; *Angew. Chem. Int. Ed.* **2011**, *50*, 9832–9837; c) F. J. Dekker, O. Rocks, N. Vartak, S. Menninger, C. Hedberg, R. Balamurugan, S. Wetzel, S. Renner, M. Gerauer, B. Scholermann, M. Rusch, J. W. Kramer, D. Rauh, G. W. Coates, L. Brunsveld, P. I. Bastiaens, H. Waldmann, *Nat. Chem. Biol.* **2010**, *6*, 449–456; d) T. Böttcher, S. A. Sieber, *Angew. Chem.* **2008**, *120*, 4677–4680; *Angew. Chem. Int. Ed.* **2008**, *47*, 4600–4603; e) Z. Wang, C. Gu, T. Colby, T. Shindo, R. Balamurugan, H. Waldmann, M. Kaiser, R. A. van der Hoorn, *Nat. Chem. Biol.* **2008**, *4*, 557–563.

[13] P. Y. Yang, K. Liu, M. H. Ngai, M. J. Lear, M. R. Wenk, S. Q. Yao, *J. Am. Chem. Soc.* **2010**, *132*, 656–666.

[14] M. Verdoes, B. I. Florea, U. Hillaert, L. I. Willems, W. A. van der Linden, M. Sae-Heng, D. V. Filippov, A. F. Kisselev, G. A. van der Marel, H. S. Overkleeft, *ChemBioChem* **2008**, *9*, 1735–1738.

